Paper # 07F-42 **Topic: Spark Ignition**

2007 Fall Meeting of the Western States Section of the Combustion Institute
Sandia National Laboratories, Livermore, CA
October 16 & 17, 2007.

Investigation of Statistical Nature of Spark Ignition

S. P. Moffett[1], *S. G. Bhanderi*[1], *J. E. Shepherd*[1], *E. Kwon*[2]

[1]*Graduate Aeronautical Laboratories (GALCIT),*
California Institute of Technology, Pasadena, California 91125-0001, USA

[2]*Electromagnetic Effects Technology, Phantom Works*
The Boeing Company, Seattle, Washington 98124-2207

Determining the minimum ignition energy (MIE) of flammable mixtures is extremely important for characterizing accidental ignition hazards in industry and in aviation. While this problem has been studied for several decades, the issue of the possible statistical nature of the ignition process itself has not been fully addressed. The MIE view prescribes a single energy threshold above which ignition occurs, whereas scatter and overlap in ignition data suggests that it may be better analyzed using statistics. In this view, the probability of ignition as a function of ignition source energy would be characterized using a probability distribution. In order to study this possible statistical nature of combustion, a highly reliable and repeatable energy source is required. In this work, a low-energy capacitive spark system is developed and characterized for use in examining MIE and the statistical nature of ignition.

1 Introduction

Determining the risk of accidental ignition of flammable mixtures is a topic of tremendous importance in industry and in aviation safety. Extensive work has been done [1–3] to determine the flammability limits of various mixtures in terms of mixture composition. These studies are all performed using a very high energy ignition source that is assumed strong enough to ignite any mixture with composition inside the flammability limits. The results are ranges of compositions for various fuels where, if a very strong ignition source is present, there is a risk of accidental ignition. However, for mixtures with compositions within the flammability limits, there also exists a limiting strength of the ignition source. If an ignition source is not strong enough, or is below the minimum ignition energy (MIE) of the particular mixture, the mixture will not ignite. Just as for flammability limits in terms of mixture composition, there have also been extensive studies to determine the minimum ignition energies of many different flammable mixtures. While the numerical modeling of the growth of a flame from a hot gas volume created by an ignition source has been considered for simple mixtures, for example Kusharin et al [4] for hydrogen-air and Maas and Warnatz [5] for hydrogen-oxygen, determining incendivity limits remains primarily an experimental issue.

In combustion science, the concept minimum ignition energy (MIE) has traditionally formed the basis of studying ignition hazards of fuels. The viewpoint is that fuels have specific ignition energy thresholds corresponding to the MIE, and ignition sources with energy below this threshold value will not be able to ignite the fuel. Standard test methods for determining the MIE have been developed [3, 6] which use a capacitive spark discharge for the ignition source. The MIE is determined from energy stored in a capacitor at a known voltage that is then discharged through a specified

gap. The pioneering work using this ignition method to determine MIE was done at the Bureau of Mines in the 1940s by Guest, Blanc, Lewis and von Elbe [7]. They obtained MIE data for many different fuels and mixture compositions, and this data is still extensively cited in the literature and ignition handbooks [3, 6]. This technique is also used to study ignition hazards in the aviation industry and standardized testing is outlined to determine the MIE of aviation test fuels [8, 9]. Since the work at the Bureau of Mines, many authors have proposed improvements on the technique for determining MIE using capacitive spark discharge, most recently Ono et al at the University of Tokyo [10, 11] and Randeberg et al at the University of Bergen [12].

One issue that makes it complicated to determine the MIE precisely is defining the spark energy. In most MIE data, the ignition energy that is reported is the energy stored in the capacitor in the discharge circuit

$$E_{stored} = \frac{1}{2}CV^2 \tag{1}$$

[7] or the energy that is discharged in the spark gap, found by subtracting the residual energy in the capacitor after the spark [10, 11]. However, only the energy that goes toward heating a critical volume of gas is important for ignition. A significant fraction of the energy stored in the capacitor does not contribute to this heating, but rather is lost to sound waves, electromagnetic radiation, visible light and IR emission and circuit losses, while some remains in the capacitor after discharge. The amount of energy lost through each of these means is unknown and extremely difficult to quantify, as it depends on the particular circuit. Therefore the MIE depends not just on the mixture composition but on the test method itself. The MIE is also found to a strong function of electrical circuit parameters, electrode construction, and spark gap width. This dependence of the MIE on the test parameters is a challenge in ignition hazard testing that has not yet been sufficiently addressed.

This view of the ignition, where the MIE is considered to be a single threshold value defined so that ignition always occurs when the ignition source is above that energy level, is the traditional viewpoint in combustion science [7] and extensive tabulations of this kind of MIE data are available [3, 6]. However, in the aviation safety industry, a different approach to ignition characterization is being used that is more consistent with experimental observations and statistical treatment of engineering test data. [9]. In standardized testing guidelines published by the FAA and SAE Aerospace Recommended Practice [8, 9] ignition is not treated as a threshold phenomenon, but rather as a statistical event. The outcome of a series of ignition tests is used to define the probability of ignition as a function of stored energy, peak current, or some other characteristic of the ignition source. It is reasonable and useful to recognize that engineering test results have inherent variability, and hence using statistical methods to analyze these variable results provides a good basis for assessing the ignition hazard of flammable mixtures.

Simple statistical methods have been applied to Jet A ignition tests performed by Lee and Shepherd at the California Institute of Technology using a standard capacitive spark discharge system as the ignition source [13]. There were 25 ignition tests performed while varying only the spark energy, and the data points were then used to derive a mean value and standard deviation for the MIE, rather than a single threshold value. This data set is used in the next section of this paper as an example to illustrate statistical analysis resulting in a probability distribution for ignition vs.

spark energy and confidence intervals. Statistical analysis of ignition data has also been applied to ignition of automotive and aviation liquid fuels as a means of assessing the risk of accidental ignition by hot surfaces [14]. Taking on the viewpoint of ignition tests as being statistical in nature raises a key question: is the statistical nature of the data due to an intrinsic characteristic of the ignition process, or is it due only to variability in the test methods? To answer this question, the experimental variability must be minimized and quantified, and an ignition source is required that is well-controlled and fully characterized.

In ignition testing there are many uncontrolled sources of variability in the experiment itself separate from the ignition energy. These uncertainties can lead to inaccurate test results and the appearance of variability in the results that has no correlation with the ignition energy. One major cause of variability in the test results is uncertainty in the mixture composition. Not only do changes in mixtures lead to changes in combustion characteristics, (flame speeds, peak pressures, etc.), as shown in the previous MIE studies [3, 6], even small changes in mixture composition can lead to large differences in MIE values. Therefore it is important to precisely control and accurately measure composition during ignition experiments. Another cause of variability is the degree of turbulence near the ignition source, as the process of flame initiation and propagation can be affected by pre-existing turbulence. Finally, a third important source of variability in the test data is the method used to detect ignition. If the detection method is unreliable or unsuitable for the combustion characteristics of the mixture being tested, a given ignition energy may be perceived as not igniting a mixture when in fact combustion did occur. Previous work has been done to assess these three sources of variability in tests involving lean H_2-O_2-Ar aviation test mixtures and to propose test methods to minimize these uncertainties [15]. The sources of uncertainty are not limited to these three, but these are major contributors to variability in the data that is unrelated to the ignition source. It is therefore necessary to quantify and minimize the uncertainties from these three sources before the variability of ignition with respect to ignition source energy can be examined.

The goal of the present work is threefold. First, statistical tools are adapted for use with ignition tests to provide a way of describing test results in terms of probabilities and confidence intervals. Secondly, a low-energy capacitive spark discharge system is designed and characterized. The data from this system can then be analyzed using the statistical tools to examine if the ignition is probabilistic or if there is simply a threshold value of the MIE. Thirdly, in this work we aim to develop test methods and an experimental setup that minimizes variability unrelated to the ignition source, specifically addressing the three sources of uncertainty described above, mixture composition, turbulence, and ignition detection. Once these three goals have been achieved, the framework exists for extensive testing of fuels to examine the nature of ignition and MIE. Ultimately, these methods will be applied to various aviation test mixtures, including hydrogen-oxygen-diluent and simple hydrocarbon mixtures, to assess their ignition hazard and accurately determine the margin of safety between these test fuels and actual jet fuel.

2 Statistical Analysis of Ignition Data

Ignition testing can be considered a sort of “sensitivity experiment,” where the goal is to measure the critical level of a stimulus that produces a certain result in a test sample. In the case of spark

ignition testing, the test sample is the combustible mixture under consideration, the stimulus level is the spark energy, and the result above the critical stimulus level is ignition of mixture. The ignition tests produce a binary outcome, where the result is either a "go" (ignition) or a "no go" (no ignition) for a given stimulus level (spark energy). It has been suggested in other work [9, 13] that when doing ignition testing with spark energies near the reported MIE, the energy levels for "go" and "no go" results overlap, giving no clear critical stimulus level (spark energy) for ignition. The overlapping of data points suggests that statistical tools are the appropriate approach to analyzing the binary test results.

2.1 Choosing Stimulus Levels: Bruceton Technique and Langlie Method

When performing ignition testing with the goal of using statistics to analyze the outcomes, it is desirable to generate data that produces meaningful statistical results with the fewest number of tests possible. Two possible methods for choosing the stimulus levels of each test are the Bruceton "Staircase" Technique (or the "Up and Down" Method) [16, 17] and the "Langlie" Method (or the "One-Shot" Method) [18], both of which were used by Lee and Shepherd when studying spark ignition of Jet A [13]. Both of these methods have the same basic requirements for the data, including that each test is performed on a new sample (i.e. a new flammable mixture), that there is a consistent criteria for determining a "go" or "no go" (i.e. pressure detection of ignition or visualization), and that the test stimuli (spark energies) are normally distributed.

For the Bruceton Technique, the minimum and maximum stimulus levels and the stimulus level increments must be chosen a priori. So if this method is applied to spark ignition tests, the minimum and maximum spark energies as well as the energy increments between tests must be determined before testing begins. The conditions of each test depend on the result of the previous test, and the dependence follows a simple rule: if a "go" is obtained on the previous test, decrease the stimulus level on the next test by one increment, and if a "no go" is obtained on the previous test, then increase the stimulus level by one increment. This method is repeated until enough data points are obtained for meaningful statistics; this method usually requires large (50-100) numbers of data points, though there is some evidence that much fewer data points can be sufficient in some cases [17].

For the Langlie Method, only the minimum and maximum stimulus levels, and not the stimulus increments, must be determined a priori. As with the Bruceton Technique, the conditions of each test depend on the result of the previous test, but by a more complicated rule. When counting backwards through the previous tests, if an equal number of "go" and "no go" results can be found, then the next stimulus level is the average of that level with equal "go"/"no go" results and the level of the last test performed. If a level with equal "go"/"no go" results after it cannot be found, then the next stimulus level is the average of the level of the last test and a limiting level (the minimum level if the last test produced a "go," and the maximum level if the last test produced a "no go"). This technique is more complicated, but using it can produce meaningful statistical results with only 10-15 data points.

2.2 Logistic Regression Method

After employing one of the two methods for choosing stimulus levels discussed in the previous section, a set of data points exists for statistical analysis. The goal is to derive a probability distribution for the probability of a "go" result (ignition) versus stimulus level (spark energy). In this work, the logistic regression method [19, 20] is used to calculate a cumulative probability distribution for the ignition data; this same statistical method has also been used for analyzing hot surface ignition of automotive and aviation fuels [14]. Once a probability distribution is obtained, percentiles and confidence intervals can also be calculated.

A binary outcome model is used for spark ignition tests with a binary result, y, where $y = 1$ for a "go" (ignition) and $y = 0$ for a "no go" (no ignition) for a given stimulus level (spark energy) x. If W is the threshold stimulus for a "go" result, then

$$y = 1 \quad \text{if} \quad W \geq x \tag{2}$$

$$y = 0 \quad \text{if} \quad W < x \tag{3}$$

Then a cumulative probability distribution for a "go" (ignition) at stimulus level x (spark energy) can be defined

$$P(x) = Probability(y = 1; x) \tag{4}$$

For n tests, all with new samples (mixtures), the following parameters are then defined:

$$x_i = \text{stimulus level (spark energy) for the } i^{th} \text{ test} \tag{5}$$

$$y_i = \text{result for the } i^{th} \text{ test } (= 0 \text{ or } 1) \tag{6}$$

$$P(x_i) = \text{probability that } y_i = 1 \text{ for the } i^{th} \text{ test} \tag{7}$$

All the stimulus levels and the binary results for the n tests are represented collectively using the likelihood function

$$L = \prod_{i=1}^{n} P(x_i)^{y_i}(1 - P(x_i))^{1-y_i}. \tag{8}$$

Then $P(x)$ can be represented with the parametric logistic distribution function

$$P(x) = \frac{1}{1 + exp(-\beta_0 - \beta_1 x)} \tag{9}$$

where β_0 and β_1 are parameters that are estimated by maximizing the likelihood function. The $100q^{th}$ percentile, x_q, can be calculated using the logistic distribution with known parameter values

$$P(x_q) = q = \frac{1}{1 + exp(-\beta_0 - \beta_1 x_q)} \tag{10}$$

and solving for x_q gives

$$x_q = (ln(\frac{q}{1-q} - \beta_0))/\beta_1. \tag{11}$$

Finally, the upper confidence limit (UCL) and lower confidence limit (LCL) for the $100(1-\frac{\alpha}{2})\%$ confidence interval for the percentile x_q can be calculated using the large sample approach for a two-sided interval

$$UCL/LCL = x_q + / - Z_{\alpha/2}\sqrt{(\sigma_{00} + 2x_q\sigma_{01} + x_q^2\sigma_{11})/\beta_1^2} \tag{12}$$

where σ_{00}, σ_{11} are the variances and σ_{01} is the covariance of β_0 and β_1, α is 1 minus the confidence level (i.e. $\alpha = 1 - 0.95 = 0.05$ for 95% confidence) and $Z_{\alpha/2}$ is the $100(1-\frac{\alpha}{2})^{th}$ percentile from a standard cumulative Gaussian distribution ($\mu = 0$, $\sigma = 1$). The result of this analysis is a cumulative probability distribution of the n spark ignition tests and a confidence envelope on the probability of ignition versus spark energy.

As an example, this statistical analysis method has been applied to Jet A ignition data at 38-39^{o}C, 0.585 bar, and a mass-volume ratio of 200 kg/m^3 obtained by Lee and Shepherd using the One-Shot method [13]. Figure 1 (a) shows the results of 25 spark ignition tests plotted versus the spark energy, and Figure 1 (b) shows the tabulated results represented in the binary form required for the statistical analysis. The likelihood function was calculated for these $n = 25$ tests, then values for β_0 and β_1 were found such that those values maximized the likelihood function. These two parameters then defined a logistic probability distribution for the data, shown in Figure 2 along with the original data points. Then, 10^{th}, 30^{th}, 50^{th}, 70^{th}, and 100^{th} percentiles were calculated using Equation 11 and the corresponding 95% confidence envelope was found by calculating the upper and lower 95% confidence limits for each percentile using Equation 12 with $\alpha = 0.05$. The resulting confidence envelope is also shown in Figure 2. While the distribution can be characterized by a mean value of spark energy, there is no single threshold value like in the MIE view of ignition.

3 Low-Energy Spark Ignition System

3.1 Design of Ignition System

In order to perform ignition testing near the MIE with the ultimate goal of performing statistical analysis on the resulting data, a well-characterized and repeatable low-energy ignition system is required. Therefore, in this work a low-energy capacitive spark ignition system has been designed and constructed, with the goal of producing small sparks with energies in the range of 100 μJ to 1 mJ. The discharge circuit is based on the ideas presented by Ono et al at the University of Tokyo [10, 11]. The basis of the design is a simple capacitive discharge circuit, but many features have been implemented to improve the system performance in terms of reliability, consistency, and repeatability so that the spark energy can be reasonably predicted and measured.

The capacitive discharge circuit consists of a Glassman model MJ15P1000 high voltage power supply (0-15 kVDC range) connected to two 50 GΩ 7.5 kV charging/isolation resistors in series with a variable vacuum capacitor (Jennings CADD-30-0115) with a range of 3 to 30 pF. The

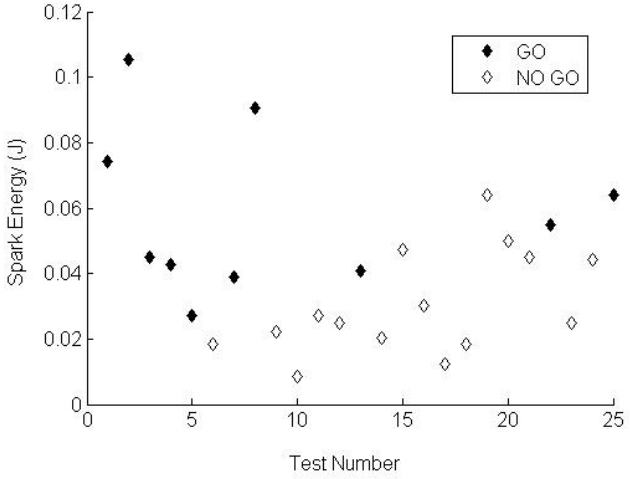

(a)

Stimulus Level (Spark Energy, J)	Binary Result (Igntion vs. None)
0.074	1
0.105	1
0.045	1
0.043	1
0.027	1
0.018	0
0.039	1
0.091	1
0.022	0
0.009	0
0.027	0
0.025	0
0.041	1
0.020	0
0.047	0
0.030	0
0.012	0
0.018	0
0.064	0
0.050	0
0.045	0
0.055	1
0.025	0
0.044	0
0.064	1

(b)

Figure 1: Jet A spark ignition data [13] shown as a plot of 25 tests versus spark energy (a) and as tabulated results in binary form (b).

capacitor is then connected in parallel with the spark gap, so that when the capacitor is charged to the gap breakdown voltage it discharges through the gap producing a small spark. The high voltage power supply output is controlled by supplying a 0-10 V input voltage provided by a function generator. The function generator outputs a ramp signal that rises from 0 to 7.32 V in 50 seconds, which causes the high voltage power supply to output a ramp of the same length increasing from 0 to 11 kV. The ramp time is chosen so that it is more than 10 times longer than the maximum capacitor charging time; therefore the output of the high voltage supply can be measured instead of directly measuring the voltage on the capacitor, since the two voltages are equal. It is important to be able to measure the voltage in this manner because of the extremely large isolation resistance; if a probe with much lower impedance is connected directly in parallel to the capacitor, a voltage divider is formed where the probe draws the majority of the current. By using a long voltage ramp to charge the resistor, it is possible to measure the capacitor voltage on the other side of the resistors. A Tektronix P6015A high voltage probe is connected to the output of the power supply to measure the capacitor voltage at breakdown, and the output is digitized by an oscilloscope at a sampling rate of 1 MS/s. The spark current is measured using a Bergoz CT-D1.0 fast current transformer, and the output is digitized by a second oscilloscope with a sampling rate 2 GS/s. The faster oscilloscope is triggered by the spark current directly, and it then triggers the second oscilloscope to record the breakdown voltage.

A high voltage relay is implemented in the circuit to disconnect the capacitor from the high voltage power supply after a spark has occurred, which is necessary to ensure that there are no multiple sparks. A Gigavac GR5MTA 15 kV load switching relay is connected between the positive output

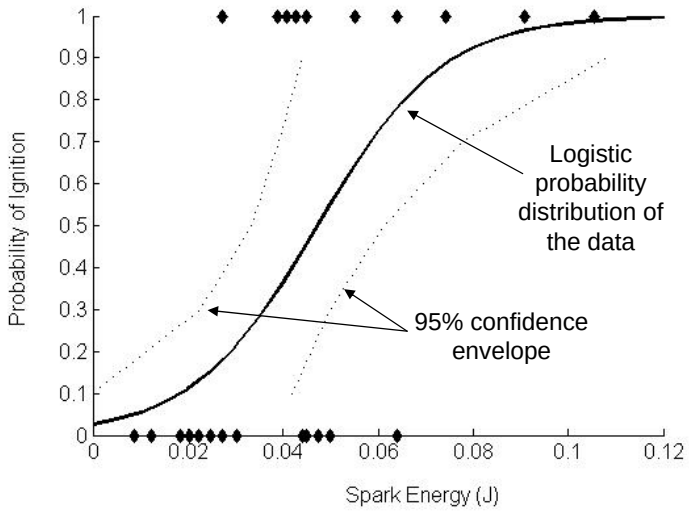

Figure 2: Logistic probability distribution and 95% confidence envelope for the Jet A spark ignition data.

of the high power supply and the first 50 GΩ charging resistor. The relay requires 12 VDC to close, which is provided by a lab power supply and a Grayhill 70-ODC5 solid state relay mounted on a Grayhill 70RCK4 rack. A timing diagram illustrating the triggering of the devices and the opening of the high voltage relay is shown in Figure 3. A 4 V power supply and a delay generator are used to provide the logic inputs to the relay; the 4 V signal leaves the relay closed during charging, so that the high voltage relay receives the 12 V signal and remains closed. When the spark begins, the current signal triggers the oscilloscope which in turn triggers the delay generator to open the solid state relay. This causes the high voltage relay to open, disconnecting the charging circuit from the high voltage ramp and preventing multiple capacitor discharges. The details of the circuit are shown in Figure 4. All the circuit components are mounted on a 0.5 in. thick acrylic plate and the resistors, capacitor, and high voltage relay are mounted on teflon standoffs to limit any leakage current. A round acrylic face plate is attached to the end of the circuit board to hold all the connections to the external power supplies, delay and function generators, and high voltage probe. All electrical connections with corners or sharp edges are coated with high voltage putty to limit corona losses.

The spark gap is constructed using two tungsten electrode tips threaded onto brass screws. The tips are 0.25 in. in diameter and turned down at one end at an angle of approximately 30^o to give a pointed tip. One of the brass screws is mounted in a piece of fiberglass held out in front of the other electrode tip on a stainless steel extender rod. The spark gap can then be adjusted by threading the brass screw further in or out through the fiberglass. The brass screw and extender arm are mounted on brass rods that feed through teflon bushings in a circular fiberglass plate, and on the other side of the plate high voltage leads are attached to the rods for connecting the spark gap to the circuit. The fiberglass plate mounts on an aluminum fixture that holds the spark gap on one side that goes inside the vessel, and the circuit board on the other side. The fiberglass plate, teflon bushings, and feed-through rods are all mounted using O-rings ensuring that the assembly is vacuum tight. As

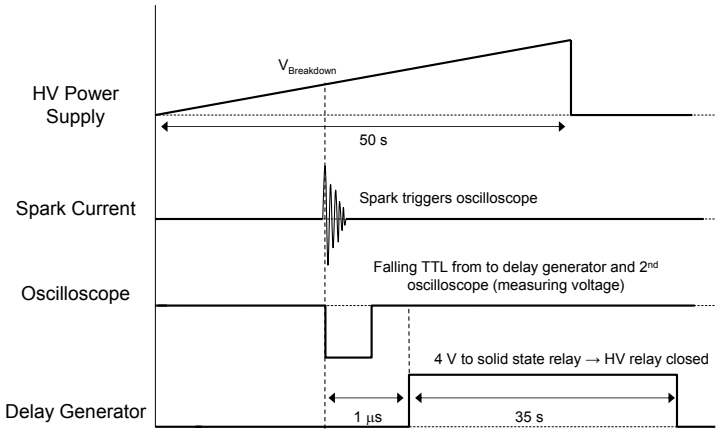

Figure 3: Timing diagram illustrating the triggering of the oscilloscope and the opening of the high voltage relay after sparking (not to scale).

with the circuit board, all sharp edges on the connections are insulated with high voltage putty. The important features of the spark gap assembly are indicated in Figure 5.

Once the circuit board has been mounted onto the aluminum fixture and the connections to the spark gap are made, an acrylic tube slides over the face plate and circuit board and sits flush with the face of the aluminum fixture. The seams between the tube and the fixture and face plate are sealed using tape and dry air is pumped through a connection in the face plate and into the enclosed circuit using a compressed air system fed through a desiccant dryer. This is necessary to keep the extremely sensitive high voltage components, particularly the capacitor surface, dry between testing, and the humidity in the circuit enclosure is monitored using a small humidity meter. Every time the tube is removed and adjustments to the circuit are made, the surfaces of the resistors, capacitor, and teflon parts are cleaned using isopropyl alcohol. The spark gap side of the aluminum fixture slides through a flange on the combustion vessel, and 4 clamps hold the fixture against the flange, forming a vacuum seal with an O-ring and providing enough force to withstand the pressure rise during ignition. A photograph of the spark ignition system mounted on the combustion vessel is shown in Figure 6.

3.2 Estimating Spark Energy

As discussed in a previous section, the traditional practice in spark ignition testing is to report the energy stored in the capacitor of the spark circuit rather than the actual energy in the spark that heats the volume of gas and initiates combustion [7]. There are other sources of energy loss, but they are extremely difficult to quantify and depend strongly on the circuit used and the test methods and will not be considered at this time. Only one source of energy loss is considered in this work, the residual energy in the capacitor after discharge. We will therefore approximate the spark energy as the difference between the original stored energy in the capacitor and the residual energy

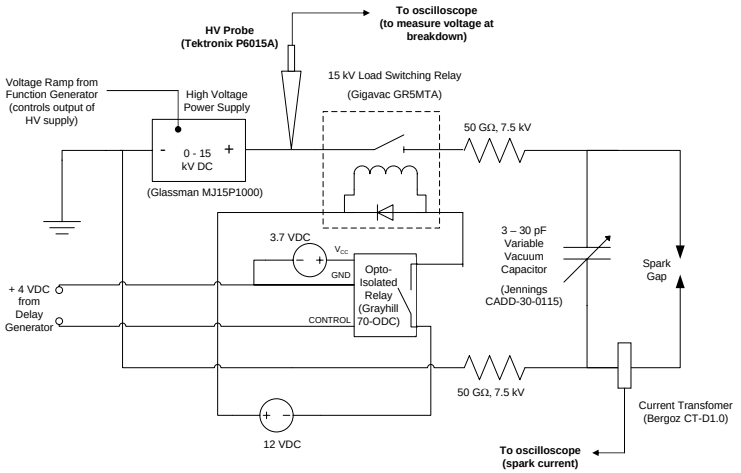

Figure 4: Schematic of the low-energy capacitive spark discharge system.

$$E_{spark} \approx E_{stored} - E_{residual} \tag{13}$$

where

$$E_{stored} = \frac{1}{2} C V_{breakdown}^2 \tag{14}$$

$$E_{residual} = \frac{1}{2} \frac{Q_{residual}^2}{C}. \tag{15}$$

The capacitance, C, is measured before the tests using an BK Precision 878A LCR meter and the voltage on the capacitor at breakdown, $V_{breakdown}$, is measured by the high voltage probe and recorded on the oscilloscope. The residual charge in the capacitor, $Q_{residual}$, can be calculated by subtracting the charge delivered in the spark from the original stored charge in the capacitor

$$Q_{residual} = Q_{stored} - Q_{spark} = C V_{breakdown} - \int i_{spark}(t) dt. \tag{16}$$

The integral of the spark current can be calculated by numerically integrating the output of the current transformer recorded by the oscilloscope. While this method of calculating the spark energy does not include the other sources of energy loss, it gives a slightly better estimate than simply using the stored energy alone. Other methods of estimating or measuring the spark energy will be investigated in future work.

4 Experimental Setup

4.1 Combustion Vessel and Filling System

The spark ignition experiments are conducted in a closed, constant-volume combustion vessel approximately 11.75 L in volume. The vessel is constructed of 1.25 in. thick steel plates that

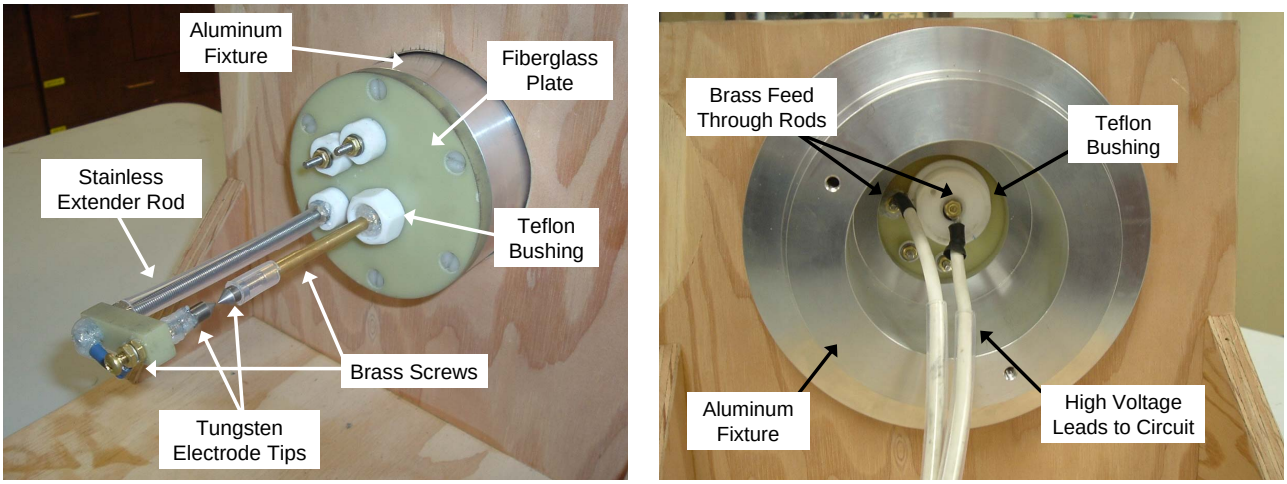

(a) (b)

Figure 5: Front (a) and back (b) views of the spark gap fixture.

form a rectangular chamber with internal dimensions of 7.48 in. x 8.0 in. x 12.0 in. Each wall has a 4.6 in. diameter port hole and bolt circle to allow different flanges to be mounted on the walls. One of the walls has a flange with a glow plug fed through it into the chamber, acting as a secondary ignition source. Two parallel walls have 1 in. thick glass windows in the port holes for visualization. On the remaining wall, the ignition system fixture is mounted in a specialized flange and held down by four aluminum clamps. The vessel lid has a fan mixer, the connection to the vacuum line, connections for gas plumbing, a pressure sensor and a thermocouple, and a septum for injecting liquid fuels.

A remotely controlled plumbing system is used to accurately fill the combustion chamber. A 1 in. ball valve separates the lab vacuum manifold from the chamber and is opened to evacuate the vessel. A gas feed line that is connected to gas bottles through a series of valves is used to fill the vessel with gases using the method of partial pressures. The static pressure is measured by a Heise 901A manometer and a precise digital readout, making it possible to fill the gases to within 0.01 kPa, giving precise mixture determination. The gas lines are also connected to the vacuum manifold so that they can be evacuated between gases to eliminate errors due to dead volume. All the valves are controlled remotely outside the experiment room. The main features of the vessel and plumbing system are shown in Figure 7.

4.2 Ignition Detection Methods and diagnostics

Three methods are used to detect the ignition and measure characteristics of the combustion. One method is a thermally-protected model 8530B Endevco piezoelectric pressure transducer used to monitor the dynamic pressure in the vessel. This is a very sensitive ignition detection method as it detects pressure changes in the vessel, and so even with modest explosion pressures, the output will clearly show the rapid pressure rise due to the combustion. The maximum pressure in the vessel and the explosion time can also be obtained from the pressure traces. A second method

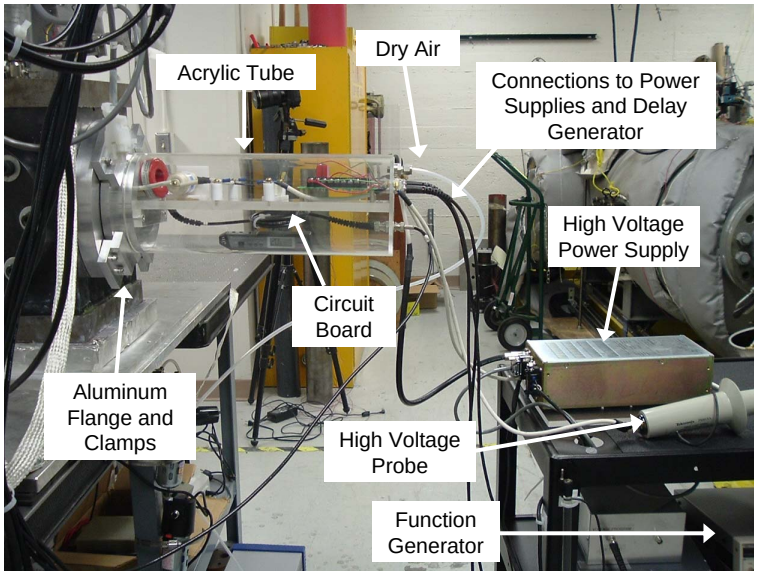

Figure 6: Low-energy spark ignition system mounted in the combustion vessel.

of ignition detection is the temperature, measured by an Omega K type thermocouple inserted through the lid of the vessel. The output of the thermocouple is converted to temperature and displayed using an Omega DP116 electronic readout. Both the dynamic pressure and temperature measurements were recorded using Labview Data Acquisition software that is triggered by the oscilloscope recording the spark current. The post-combustion pressure of the products was also recorded using the Heise gauge. The third method of ignition detection was visualization of the flame through the vessel windows using a simple schlieren system, a schematic of which is shown in Figure 8. The schlieren system uses a pulsed LED light source constructed using a Luxeon LXHL-LW6C LED connected to a simple capacitor discharge circuit that is triggered using a TTL signal to an IRL 540N MOSFET. The light pulse from the LED is directed through a collimating lens and aperture before reaching the vessel. After the vessel, the light is focused on a horizontal knife edge and the schlieren image of the flame is recorded on a Sumix 150 CMOS camera. The image is a close-up view of the spark gap with resolution 1280 x 1024 and a field of view of approximately 12.7 mm x 11 mm. The timing of the light pulse determines the time the image is taken, and the triggering of the LED circuit as well as the camera shutter are achieved using a second delay generator that is triggered by the delay generator in the spark ignition system.

5 Results

5.1 Preliminary Spark Characterization

The low-energy spark ignition system has been operated multiple times to examine qualitatively its operation and repeatability. To study the lower limit of the spark energy, the variable capacitor was turned to its lowest setting of approximately 3 pF and the capacitance was measured at by attaching the leads of the LRC meter to the ends of the isolation resistors. Performing the measurement at this location in the circuit gives the total capacitance that contributes to the stored energy, including

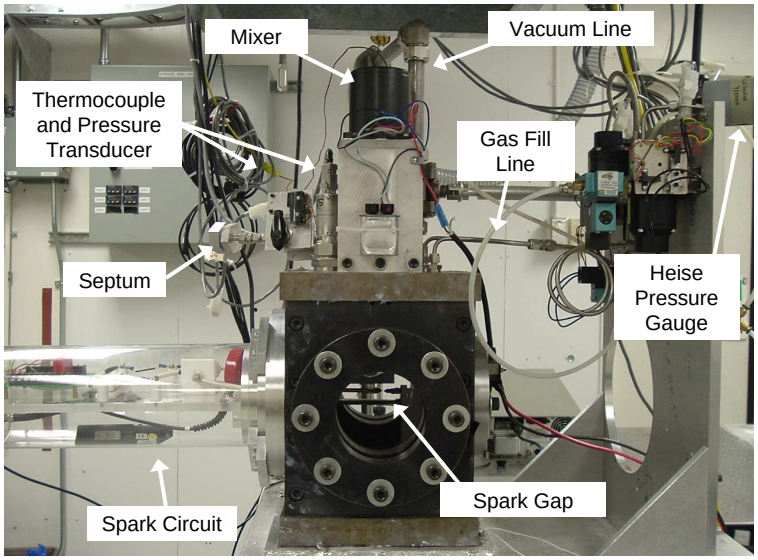

Figure 7: Combustion vessel and main features of the gas plumbing system.

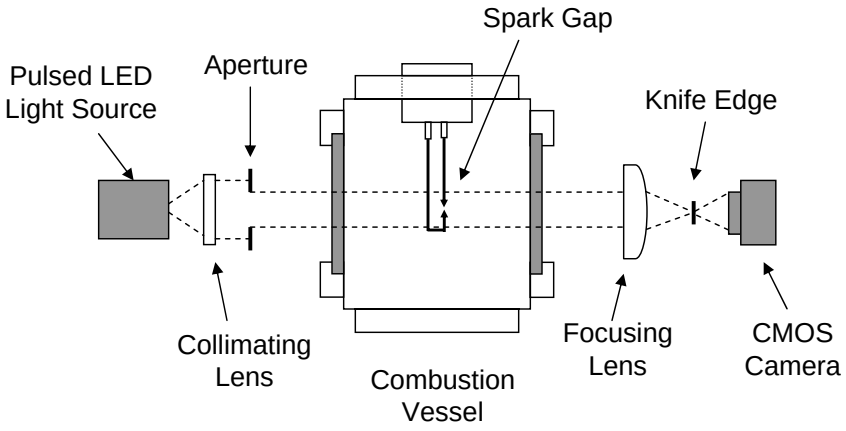

Figure 8: Schematic of the schlieren system used for flame visualization.

the stray capacitance due to the circuit connections and spark gap, which in this case is on the same order as the capacitor. The spark gap was set to approximately 1 mm, and the spark system was then triggered 10 consecutive times, producing one single spark each time. The spark current and breakdown voltage were recorded on the oscilloscope, and the current waveforms of the 10 independent sparks are shown in Figure 9. Qualitatively, the waveforms all appear to have the same trend and similar peak current levels; all the sparks are on the order of 50 ns in length and the peak currents are all between approximately 4.8 and 6.8 amps.

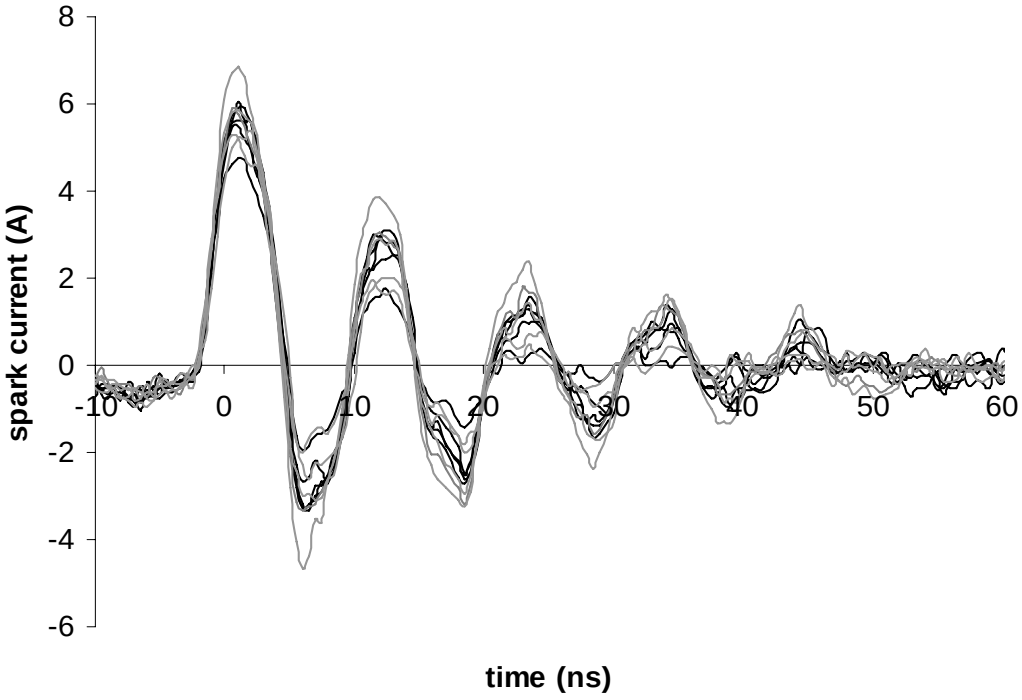

Figure 9: Current waveforms for 10 consecutive, independent sparks (C$= 7.0$ pF).

The spark energies were estimated using Equations 13-16. The total capacitance was measured as 7.0 pF, and the breakdown voltages were obtained from the voltage signals recorded on the oscilloscope and used to calculate the stored energy. To estimate the spark charge, the spark current waveforms were integrated numerically using the Trapezoidal rule from breakdown at $t \approx -2$ ns to $t = 50$ ns where the oscillation amplitudes have been damped to less than 90% of the peak current. An interval width of 0.5 ns was used in the integration since the waveform was digitized at a sample rate of 2 GS/s. The spark energies were then estimated to be between 50 and 60 μJ and these values, along with the results of the intermediate calculations and the mean and standard deviation values, are shown in Table 1. While this preliminary characterization verified the operation of the circuit at extremely low capacitances and showed that the sparks are fairly consistent, further characterization is clearly necessary to fully assess the operation of the ignition system. To accurately characterize the system, a criteria for choosing the "cut-off" point in the integration of the spark current must be chosen, and statistical tools must be implemented to properly analyze the repeatability of the spark energies. Also, the system should be tested over a

range of energies and breakdown voltages by varying the capacitance and the spark gap. Additional changes may also be made to improve the consistency of the sparks, such as a new electrode design.

Table 1: Charge and energy estimates for 10 consecutive sparks with C = 7.0 pF and a spark gap of approximately 1 mm.

	Spark Number										Mean	Standard Deviation
	1	2	3	4	5	6	7	8	9	10		
$V_{breakdown}$ (kV)	4.4	4.4	4.4	4.4	4.4	4.4	4.4	4.6	4.4	4.4	4.42	0.06
Q_{stored} (nC)	30.8	30.8	30.8	30.8	30.8	30.8	30.8	32.2	30.8	30.8	30.9	0.42
E_{stored} (μJ)	68	68	68	68	68	68	68	74	68	68	68.6	1.8
Q_{spark} (nC)	15.7	17.1	17.6	16.0	15.9	15.7	16.1	18.0	15.3	17.5	16.5	0.91
$Q_{residual}$ (nC)	15.1	13.7	13.2	14.8	14.9	15.1	14.7	14.2	15.5	13.3	14.4	0.75
$E_{residual}$ (μJ)	16.3	13.5	12.4	15.7	15.9	16.3	15.3	14.3	17.1	12.7	14.9	1.5
E_{spark} (μJ)	51.5	54.3	55.3	52.1	51.9	51.5	52.4	59.7	50.7	55.1	53.7	2.5

5.2 Flame Visualization

Preliminary tests using the low-energy spark system at the upper limit of its spark energy were performed to verify ignition capabilities of the system. The flammable mixture used was an aviation test mixture of 7% H_2, 21% O_2, and 72% Ar described in FAA aircraft safety guidelines [9]. The capacitor was turned up to its maximum value giving a total capacitance of approximately 34.1 pF and the spark gap was set to 1.5 mm; the resulting sparks were on the order of 1 mJ, which is significantly higher than the theoretical MIE for similar mixtures [7]. A set of 7 tests were performed and ignition was observed in all the tests by the three detection methods described in Section 4. The pressure and temperature rise due to ignition were clearly detected by the pressure transducer and thermocouple, as can be seen in the traces in Figure 10. Visualization of the flame was also achieved using the schlieren system described in Section 4. The images were taken at different times during the initiation and subsequent propogation of the flame by controlling the timing of the pulse from the LED light source. The camera exposure was set to 0.5 ms, and was triggered between 25 and 100 μs before the 5 μs LED pulse. Over the 7 ignition tests, the LED pulse delay time was increased from 25 μs to 2 ms to obtain a series of images of the flame evolution in time, shown in Figure 11.

5.3 Approximating the Ignition Threshold

Ignition tests were performed on the H_2-O_2-Ar mixture described in the previous section using the low-energy spark ignition system at the minimum and maximum capacitance settings with a spark gap of 1 mm. The lower energy spark, on the order of 50 μJ, did not ignite the mixture, while the higher energy spark, on the order of 300 μJ, did ignite the mixture. Obtaining a “go” and a “no go” within the range of the spark ignition system implied that the ignition threshold, whether it

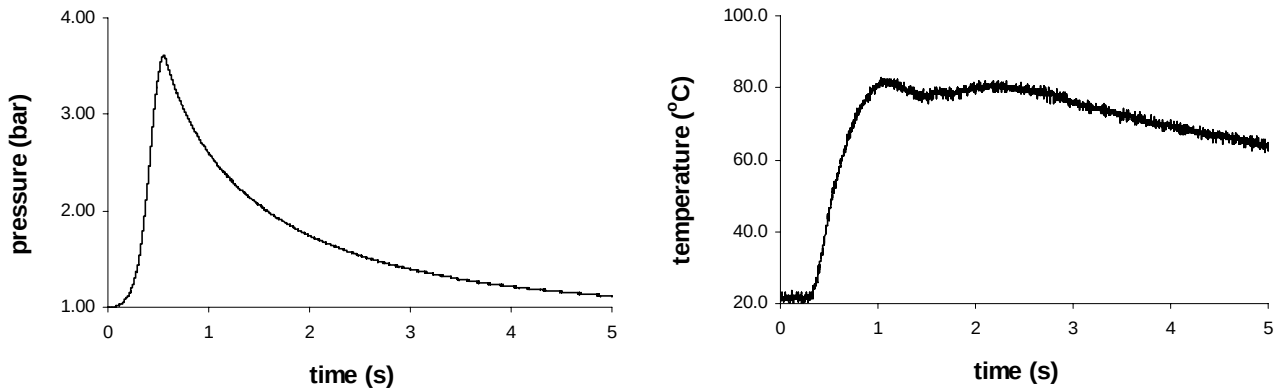

Figure 10: Pressure (a) and temperature (b) measured during ignition of an H_2-O_2-Ar mixture using the low-energy capacitive spark system.

is a single value (MIE) or a probability distribution, lies in this range. A short set of 10 ignition tests with estimated spark energies ranging from 40 to 150 μJ were then performed in an attempt to bracket the ignition energy range.

The results of the 10 ignition tests are shown in Figure 12, with the binary results of the ignition tests (0 for a "no go"/no ignition, 1 for a "go"/ignition) plotted versus the stored energy (Figure 12 (a)) and the estimated spark energy (Figure 12 (b)). The five sparks with energies at and above 86 μJ all ignited the mixture, while four sparks with energies at and below 73 μJ did not cause ignition. This suggests that the spark energy threshold lies between 73 and 86 μJ, corresponding to a stored energy range of approximately 86 to 102 μJ. This result can be compared to the expected value of the MIE for a similar mixture from the early work at the Bureau of Mines, as presented by Lewis and von Elbe (Figure 164) [7]. They present MIE data for mixtures with a constant ratio of oxygen to diluent, $O_2/(O_2 + \text{inert gas}) = 0.21$ and varying hydrogen concentration. There is a curve for mixtures with argon as the diluent gas, and for 7% H_2 the MIE is given as approximately 100 μJ. Note that this value is not the spark energy, but rather the stored energy in their capacitive discharge system; the actual spark energy would be lower. For the mixture used in this work, the oxygen to diluent ratio is slightly larger, $O_2/(O_2 + \text{inert gas}) \approx 0.226$, so it is expected that our MIE value would be slightly lower than the value given by Lewis and von Elbe. The results of this work, as stated above, suggest a stored energy threshold range of about 86 to 102 μJ, which is consistent with what we would expect based on the previous work. However, it is important to note that ignition occurred with one spark with an estimated energy on the order of 60 μJ, and this is a contradictory data point. Whether this contradiction is a result of an inherent statistical nature of ignition or variability in the test method is unknown, and clearly a much larger number of tests are required to precisely determine the ignition energy range. However, this small set of tests illustrates the need for further ignition testing using test methods that minimize variability and a fully characterized low-energy ignition system.

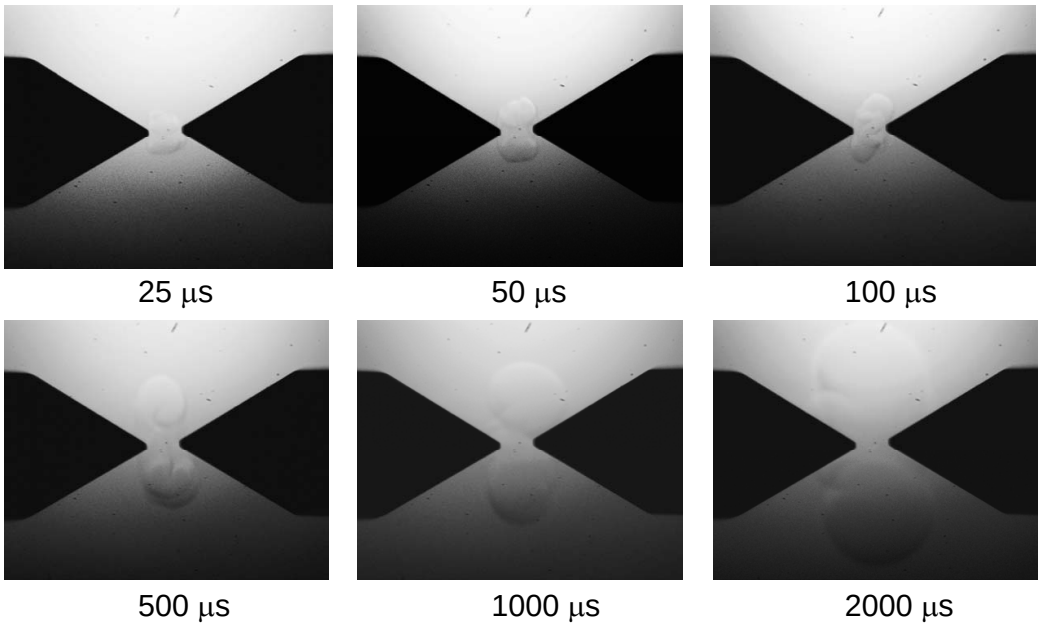

Figure 11: Schlieren images of flame initiation and propagation from 25 μs after the spark to 2 ms.

6 Concluding Remarks

The traditional view of ignition is that there exists a minimum ignition energy (MIE), a single threshold value above which ignition always occurs and below which ignition cannot occur. However, in recent work the view of ignition as a probabilistic event has been proposed [8, 9, 13, 14]. In this view there does not exist a single well-defined threshold energy value, but rather a probability distribution of ignition versus ignition energy and so ignition test results should be analyzed using statistical tools. Treating ignition testing in this manner may be more appropriate given the variability in ignition test results near the MIE, but this issue remains unresolved. The question remains of whether ignition is inherently statistical in nature or if the perceived variability in the test results is due to variability in the test methods. The goal of this and future work is to develop and characterize a low-energy ignition capacitive spark ignition system that can produce repeatable sparks near the reported MIE values of aviation test mixtures, on the order of 100 μJ. Also, this work aims to design an experiment that minimizes, as much as possible, the variability in the test results due to the test methods, and to quantify any remaining uncertainties.

The low-energy capacitive spark ignition system has been designed and constructed. Preliminary characterization of the spark energy has been performed at the lower limit of the spark system energy range, successfully producing sparks with energies near 100 μJ. A scheme for estimating the spark energy based on spark current measurements was used to estimate the spark energies. The ignition capabilities of the system were also confirmed by producing the sparks with the highest capacitance setting in a lean H_2-O_2-Ar test mixture. Ignition was confirmed in all 7 tests by three reliable detection methods, and pressure and temperature traces as well as schlieren visualization of the flame initiation were obtained. In addition, a range for the ignition energy threshold was investigated for the test mixture by varying the energy of the spark ignition system through chang-

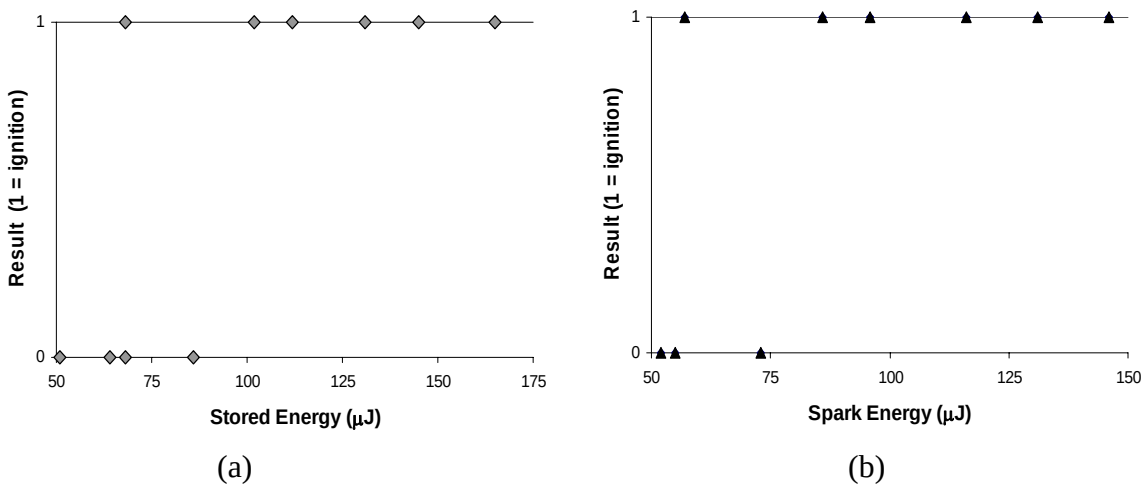

Figure 12: Results of 10 ignition tests performed using the low-energy spark ignition system plotted versus stored energy (a) and estimate of the spark energy (b). The result is "0" if no ignition occurs and a "1" if ignition does occur.

ing the capacitance. A short set of 10 ignition tests were performed in this manner, and while 9 of the results implied an ignition energy threshold between approximately 73 and 86 μJ and a stored energy range consistent with previous work [7], a contradictory data point was obtained. This investigative test series reinforced the need for further testing in a highly controlled experimental environment.

The results presented in this work represent the first stage of the development of a method for evaluating the nature of ignition and determining whether ignition is a threshold or probabilistic event. More work is required to fully characterize the spark ignition system, including setting specific criteria for the calculation of the spark charge, i.e. determining bounds on the current integration. Once the criteria is determined, a series of tests will be performed while varying capacitance and spark gap, and the estimated spark charges and energies will be analyzed statistically to quantify spark repeatability. Small further improvements on the ignition system will also be made, including improving the spark gap construction. Other methods of estimating or measuring the spark energy may also be implemented, such as sensitive calorimetry, using laser diagnostics to determine gas kernel temperature, etc. Improvements will also be made to the experimental setup and test methods. A full assessment of the experimental uncertainties and the effects on the test results will be done, and all devices used in the testing will be recalibrated to ensure accurate mixture composition and ignition detection. The test methods will be addressed and finalized to ensure repeatability and precision of the ignition testing, including possibly programming a computer to perform the tests to minimize variability due to human error. This future work will culminate in ignition testing near the reported MIE values of various H_2-based aviation test fuels as well as hydrocarbon fuels to examine the possible statistical nature, and eventually testing actual jet fuel for comparison with the test mixtures.

Acknowledgments

The authors would like to thank Raza Akbar for his help with the flame imaging. The experimental work was carried out in the Explosion Dynamics Laboratory of the California Institute of Technology and was supported by The Boeing Company through a Strategic Research and Development Relationship Agreement CT-BA-GTA-1.

References

[1] L. G. Britton. *Process Safety Progress*, 21 (2002) 1–11.

[2] H. F. Coward and G. W. Jones. The limits of flammability of gases and vapors. Technical report, 1952. Bulletin 503, Bureau Mines.

[3] V. Babrauskas. *Ignition Handbook: Principles and Applications to Fire Safety Engineering, Fire Investigation, Risk Management and Forensic Science*. Fire Science Publishers, Issaquah, WA, 2003.

[4] A. Yu. Kusharin, O. E. Popov, G. L. Agafonov, and B. E. Gelfand. *Experimental Thermal and Fluid Science*, 21 (2000) 2–8.

[5] U. Maas and J. Warnatz. *Combustion and Flame*, 74 (1988) 53–69.

[6] E. C. Magison. *Electrical Equipment in Hazardous Locations*. Instrument Society of America, 3rd edition, 1990.

[7] B. Lewis and G. von Elbe. *Combustion, Flames and Explosions of Gases*. Academic Press, New York, 1961.

[8] Anonymous. Aerospace recommended practice aircraft lightning test methods. Technical report, 2005. SAE Aerospace Report ARP5416.

[9] Anonymous. Aircraft fuel system lightning protection design and qualification test procedures development. Technical report, 1994. U.S. Dept. of Transportation Federal Aviation Administration Report DOT/FAA/CT-94/74.

[10] R. Ono, N. Masaharu, S. Fujiwara, S. Horiguchi, and T. Oda. *Journal of Applied Physics*, 97 (2005) 123307.

[11] R. Ono, N. Masaharu, S. Fujiwara, S. Horiguchi, and T. Oda. *Journal of Electrostatics*, 65 (2007) 87–93.

[12] E. Randeberg, W. Olsen, and R. K. Eckhoff. *Journal of Electrostatics*, 64 (2006) 263–272.

[13] J. J. Lee and J. E. Shepherd. Spark energy measurements in jet a part II. Technical report, Graduate Aeronautical Laboratories, California Institute of Technology, Pasadena, CA, 1999. Explosion Dynamics Laboratory Report FM 99-7.

[14] J. Colwell and A. Reza. *Fire Technology*, 41 (2005) 105–123.

[15] E. Kwon, S. P. Moffett, J. E. Shepherd, and A. C. Day. *International Conference on Lightning and Static Electricity*, (2007) PPR–48.

[16] J. Zukas and W. Walters, editors. *Explosive Effects and Applications*, chapter 8: Hazard Assessment of Explosives and Propellants. Springer-Verlag NY, 1998.

[17] W. J. Dixon and F. J. Massey Jr. *Introduction to Statistical Analysis*. McGraw-Hill, 1983.

[18] H. J. Langlie. A test-to-failure program for thermal batteries. In *Sixteenth Annual Power Sources Conference*. PSC Publications Committee, 1962.

[19] D. Hosmer and S. Lemeshow. *Applied Logistic Regression*. John Wiley and Sons, 1989.

[20] J. Neter, M. H. Kutner, W. Wasserman, and C. J. Nachtsheim. *Applied Linear Statistical Models*. McGraw-Hill/Irwin, 4th edition.